ELSEVIER

Contents lists available at ScienceDirect

# Carbohydrate Polymers

journal homepage: www.elsevier.com/locate/carbpol





# Ulvans are not equal - Linkage and substitution patterns in ulvan polysaccharides differ with *Ulva* morphology

Joel T. Kidgell<sup>a,b,\*</sup>, Christopher R.K. Glasson<sup>c</sup>, Marie Magnusson<sup>c</sup>, Ian M. Sims<sup>b</sup>, Simon F.R. Hinkley<sup>b</sup>, Rocky de Nys<sup>a</sup>, Susan M. Carnachan<sup>b</sup>

- <sup>a</sup> College of Science and Engineering, James Cook University, Townsville 4811, Australia
- b The Ferrier Research Institute, Victoria University of Wellington, Wellington 6012, New Zealand
- <sup>c</sup> School of Science, University of Waikato, Tauranga 3110, New Zealand

#### ARTICLE INFO

Keywords:
Seaweed
Ulva
Ulva
Structure
Methylation analysis
Gas chromatography—mass spectrometry
Nuclear magnetic resonance spectroscopy

#### ABSTRACT

Ulva are hardy green seaweeds that contain the sulfated polysaccharide ulvan and grow in two distinct morphologies: foliose and tubular. The authors hypothesise that ulvan from tubular species are more structurally complex than ulvans from foliose species. Herein, using standardised methods, the glycosyl linkage positions and sulfate ester substitutions of constituent monosaccharides of ulvan isolated from foliose (U. lacinulata and U. stenophylloides) and tubular (U. prolifera and U. ralfsii) species of Ulva were investigated. Comparison of native ulvans with 80 and 100 °C desulfated counterparts indicated that 4-linked rhamnose is predominantly 3-0-sulfated in all four ulvans. Ulvans from the foliose species predominantly contained  $\rightarrow$ 3,4)-Rhap- $(1\rightarrow, \rightarrow 4)$ -GlcAp- $(1\rightarrow \text{and} \rightarrow 4)$ -IdoAp- $(1\rightarrow, \text{collectively}$  accounting for 67 to 81 mol% of the total linkages. In contrast, these same linkages in ulvans from te tubular species only collectively accounted for 29 to 36 mol%. Instead, ulvan from tubular species contained a combination of  $\rightarrow$ 2,3,4)-Rhap- $(1\rightarrow, \text{terminal Rhap-}(1\rightarrow, \rightarrow 4)$ -GlcAp- $(1\rightarrow, \rightarrow 4)$ -Xylp- $(1\rightarrow, \text{and/or} \rightarrow 4)$ -Glap- $(1\rightarrow \text{in high proportions};$  some of the latter three residues were also likely 0-2 sulfated. The results presented here suggest that ulvan from foliose species are predominantly unbranched polysaccharides composed of repeat disaccharides while ulvans from tubular species contain a greater diversity of branch and sulfate substitution locations.

#### 1. Introduction

Ulva are hardy green seaweeds (marine macroalgae) with high growth rates and high proportions of bioactive sulfated polysaccharides. Species of Ulva occur in two distinct morphologies: a flat sheet-like foliose form, and a filamentous tubular form. The morphological distinction between foliose and tubular species of Ulva is so pronounced that many tubular species were considered a separate genus, Enteromorpha, until genetic analysis consolidated them into the Ulva genus (Hayden et al., 2003). Both morphologies are targets for a broad range of applications including human and animal feed products, nutraceuticals,

bioremediation, and production of the bioactive sulfated poly-saccharide, ulvan (Kidgell, Magnusson, de Nys, & Glasson, 2019; Lawton, Sutherland, Glasson, & Magnusson, 2021).

Ulvans are sulfated cell wall polysaccharides predominantly composed of rhamnose, glucuronic acid, iduronic acid and xylose (Kidgell et al., 2019). These sugars occur primarily as 4-linked repeat disaccharides: ulvanobiuronic acid type  $A_{3S}$ ,  $(\rightarrow 4)-\beta$ -D-GlcpA- $(1\rightarrow 4)-\alpha$ -L-Rhap3S- $(1\rightarrow)$ , and  $B_{3S}$ ,  $(\rightarrow 4)-\alpha$ -L-IdopA- $(1\rightarrow 4)-\alpha$ -L-Rhap3S- $(1\rightarrow)$ , and ulvanobiose  $U_{3S}$ ,  $(\rightarrow 4)-\beta$ -D-Xylp- $(1\rightarrow 4)-\alpha$ -L-Rhap3S- $(1\rightarrow)$  (Lahaye & Robic, 2007). Additional repeat structures with  $\beta$ -D-GlcpA as a branch at O-2 of Rhap3S residues and sulfation at O-2 of Xylp residues have also

Abbreviations: GlcpA, glucuronopyranosic acid; IdopA, iduronopyranosic acid; Rhap, rhamnopyranose; Rhap3S, rhamnopyranose-3-sulfate; Xylp, xylopyranose; Glcp, glucopyranose; Galp, galactopyranose; MES, 2-(N-morpholino)-ethanesulfonic acid; TFA, trifluoroacetic acid; PMAA, partially methylated alditol acetate; 2,3,4-Rha, 1,5-di-O-acetyl-1-deuterio-2,3,4-tri-O-methylrhamnitol (other derivatives are similarly abbreviated);  $\rightarrow$ 2,3,4)-Rhap-( $1\rightarrow$ , 2,3,4-tri-O-methylrhamnopyranose (other derivatives are similarly abbreviated); MWCO, molecular weight cut-off.

<sup>\*</sup> Corresponding author at: College of Science and Engineering, James Cook University, Townsville 4811, Australia.

*E-mail addresses*: joel.kidgell@my.jcu.edu.au (J.T. Kidgell), christopher.glasson@waikato.ac.nz (C.R.K. Glasson), marie.magnusson@waikato.ac.nz (M. Magnusson), ian.sims@vuw.ac.nz (I.M. Sims), simon.hinkley@vuw.ac.nz (S.F.R. Hinkley), rocky.denys@jcu.edu.au (R. de Nys), susie.carnachan@vuw.ac.nz (S.M. Carnachan).

been identified (Lahaye & Ray, 1996). Notably, the majority of sulfation is reported to occur on *O*-3 of Rhap (Ray & Lahaye, 1995). The order of the disaccharides, total size (molecular weight) of the polysaccharide, degree of sulfation, and other structural components of the molecule all influence the bioactivity of ulvan (Kidgell et al., 2019). Elucidation of the detailed structure of ulvan using NMR and linkage (methylation) analysis has involved a limited number of *Ulva* species. Most of these studies investigated ulvan from a single species, including the tubular species, *U. compressa* (Chattopadhyay et al., 2007; Lopes et al., 2017) and *U. intestinalis* (Gosselin, Holt, & Lowe, 1964), and foliose species, *U. rigida* (Ray & Lahaye, 1995) and *U. lactuca* (Brading, Georg-Plant, & Hardy, 1954; Medcalf, Lionel, Brannon, & Scott, 1975). Comprehensive assessments of the composition and structure of ulvans from multiple species and morphologies of *Ulva* have been conducted in recent years (Glasson et al., 2022; Kidgell et al., 2020).

A recent comparison of purified ulvans isolated from eight species of Ulva from Aotearoa New Zealand found the composition and rheology of ulvans from foliose species were significantly different to those from tubular species (Kidgell et al., 2020). Ulvans from tubular species had higher weight average molecular weight (M<sub>w</sub> = 260-406 kDa), formed gels with higher storage moduli (G' = 22.7-74.2 Pa), and contained less iduronic acid (IdoA = 4-7 mol%) compared to foliose species ( $M_w =$ 190–254 kDa; G' = 0.1–6.6 Pa; IdoA = 7–18 mol%). NMR spectroscopy indicated there were also morphology-based differences in the fine structure (glycosidic linkage and sulfation pattern) of these ulvans, with the spectra of ulvans from tubular species displaying greater signal complexity, indicative of a more heterogeneous structure, compared to foliose species (Kidgell et al., 2020). Glasson et al. (2022) reported similar structural differences between ulvans from tubular and foliose species of Ulva collected from different geographical regions and cultivation conditions. Ulvan from U. ohnoi (foliose species) contained a high proportion of the  $(\rightarrow 4)$ - $\beta$ -D-GlcpA- $(1 \rightarrow 4)$ - $\alpha$ -L-Rhap3S- $(1 \rightarrow)$  repeat unit, whereas ulvans from tubular U. tepida and U. prolifera appeared to be either more highly branched or sulfated, and contained more galactose (Glasson et al., 2022).

Based on this previous research, the authors hypothesise that ulvans from tubular species of *Ulva* are more structurally complex than ulvans from foliose species. To investigate this hypothesis, the glycosyl linkage positions and sulfate ester substitutions of component monosaccharides from four ulvans were identified and quantified. The four ulvans assessed, two from foliose species (*U. lacinulata* and *U. stenophylloides*) and two from tubular species (*U. prolifera* and *U. ralfsii*), were isolated using standardised conditions and were characterised previously (Kidgell et al., 2021). The aims of this study were to: (I) identify differences in the glycosyl linkage composition of ulvans isolated from foliose and tubular species of *Ulva*, and (II) determine the position and extent of sulfation of monosaccharide constituents of ulvans from the different *Ulva* morphologies.

#### 2. Methods

#### 2.1. Materials

The following were purchased from Sigma-Aldrich: anhydrous pyridine (#270970), anhydrous DMSO (#276855), anhydrous methanol (#322415), hydrochloric acid (#258148), 2-(N-morpholino)-ethane-sulfonic acid (MES, #M8250), potassium hydroxide (#221473), N-Cyclohexyl-N'-(2-morpholinoethyl)carbodiimide methyl-p-toluenesulfonate (#C106402), sodium borodeuteride (#205591), 2-amino-2-(hydroxymethyl)-1,3-propanediol (Tris base #T1503), glacial acetic acid (#695092), triethylamine (#471283), dimethyl sulfoxide (DMSO, #276855), iodomethane (#289566), ammonium hydroxide (#221228), methanol (#322415), ethyl acetate (#34858), acetic anhydride (#91204), dichloromethane (DCM, #34856), sodium carbonate (#222321), sodium nitrate (>99.0 %, #S5506), and sodium azide (>99 %, #S2002).

Other reagents were sourced as follows: trifluoroacetic acid

(synthesis grade, Scharlau, Spain, #AC31420100), sodium hydroxide (50 % *w*/w, Fisher Scientific, Thermo Fisher Scientific, New Zealand, #SS254), perchloric acid (BDH Chemicals, #87003), acetic acid (Fisher Scientific, #A38S), *myo*-inositol (research grade, Serva, Germany, #26310).

Purified ulvans isolated from Aotearoa New Zealand *Ulva* as described in Kidgell et al. (2021) were used. Ulvans isolated from *U. prolifera* and *U. ralfsii* (cult.) were chosen as they had higher than median (Kidgell et al., 2019) proportions of rhamnose (60 mol%) and galactose (16 mol%), respectively. Ulvan isolated from *Ulva lacinulata* (reported as *U. rigida* in Kidgell et al. (2021), the name has since been changed (Hughey, Gabrielson, Maggs, & Mineur, 2022)) was chosen for its high proportion of iduronic acid (18 mol%). Ulvan from *Ulva stenophylloides* (reported as *U. sp. B* (cult. B) in Kidgell et al. (2021), the name has since been changed (Nelson, D'Archino, Neill, & Robinson, 2021)) was included to represent the more 'conventional' sugar composition of ulvan. Note that in Kidgell et al. (2021) foliose and tubular species were referred to as "blade" and "filamentous", respectively.

#### 2.2. Derivatisation and linkage analysis

The glycosyl linkage compositions of the four ulvans were determined by methylation analysis following solvolytic desulfation and reduction of uronic acid residues to their dideuterio-labelled neutral sugars.

#### 2.2.1. Desulfation

Solvolytic desulfation of native ulvans was carried out based on methods previously described (Nagasawa, Inoue, & Tokuyasu, 1979; Usov, Adamyants, Miroshnikova, Shaposhnikova, & Kochetkov, 1971), with some modifications. Ulvans were converted to the pyridinium salt form by dialysing (MWCO 6–8 kDa) against 10 volumes of 0.1 M pyridine-HCl (pH 7) three times, followed twice by Type 1 water, each for 8–12 h. The pyridinium salt forms were then dissolved (2.5 mg mL<sup>-1</sup>) in an anhydrous mixture of DMSO-methanol-pyridine (89:10:1) under an atmosphere of argon in a sealed Kimax tube and heated (80 °C or 100 °C, 4 h) in a dry block heater. Once cooled, the solution was dialysed (6–8 kDa) against Type 1 water four times, for 8–12 h each, and the desulfated ulvan recovered by freeze drying. The extent of desulfation was evaluated by Fourier transform infrared spectroscopy (FTIR), monitoring the S=O bond at ~1250 cm<sup>-1</sup> (see supplementary data for more detailed information).

#### 2.2.2. Carboxyl reduction

Native and desulfated (80 °C or 100 °C) ulvans were carboxyl reduced using a modification of Sims and Bacic (1995). Ulvans (5 mg) dissolved in MES-KOH (2.5 mL, 30 mM, pH 4.75) were sonicated in an ice bath (30 mins) following addition of *N*-cyclohexyl-*N*-(2-morpholineoethyl) carbodiimide *metho-p*-toluensulfonate (400  $\mu$ L, 500 mg mL $^{-1}$ ) before heating to 30 °C for 3 h. The activated residues were reduced with sodium borodeuteride (NaBD<sub>4</sub>; 1 mL, 70 mg mL $^{-1}$  in 0.05 M NaOH) for 18 h at 25 °C, buffered with Tris-HCl (1 mL, 2 M, pH 8.0). The remaining reductant was neutralised with glacial acetic acid (1–10 drops) prior to dialysis (molecular weight cut-off 6–8 kDa) against Type 1 water (three times, 24 h each). Carboxyl-reduced samples were recovered by freeze drying. The carboxyl reduction procedure was repeated 2–3 times, until the uronic acid content was <5%w/w as determined by constituent sugar analysis using HPAEC-PAD (Nep et al., 2016).

#### 2.2.3. Methylation analysis

Carboxyl reduced ulvans were methylated using a modified method based on Ciucanu and Kerek (1984). To increase solubility in DMSO, samples were converted to the triethylammonium (TEA) salt form by exhaustive dialysis against triethylamine-HCl (0.1 M, pH 7.0) followed by Type 1 water and recovered by freeze drying (Stevenson & Furneaux,

1991). The TEA salt forms (0.5 mg, in duplicate) dissolved in DMSO (200  $\mu L)$  were combined with freshly prepared NaOH/DMSO slurry (200  $\mu L$ ;  $\sim \! 120$  mg NaOH pellets ground in 1 mL DMSO) and iodomethane (3  $\times$  50  $\mu L$  aliquots interspaced with 30–60 min sonication/stirring). Type 1 water (2 mL) and glacial acetic acid (100  $\mu L$ ) were added prior to exhaustive dialysis (MWCO 6–8 kDa) against 10 volumes of Type 1 water until the conductivity of the dialysate was  $< \! 1 \, \mu S \, cm^{-1} \! .$  Per-O-methylated ulvans were recovered by freeze drying and methylated a second time.

Partially methylated alditol acetates (PMAAs) were prepared from the per-O-methylated, carboxyl reduced ulvans using a method based on Harris, Henry, Blakeney, and Stone (1984). The permethylated polysaccharides were hydrolysed (2.5 M TFA, 1 h, 121 °C), dried, and myoinositol (10 µg) added as an internal standard. The samples were reduced (1 M NaBD4 in 2 M NH4OH, 18 h, 25 °C; excess NaBD4 neutralised by glacial acetic acid after 18 h) followed by the iterative addition and evaporation to dryness of acetic acid in methanol (5 %  $\nu/\nu$ ,  $2 \times 500 \ \mu L)$  and methanol (2–4  $\times$  500  $\mu L)$  until the dried sample appeared crystalline. The partially methylated alditols were then acetvlated by adding glacial acetic acid (40 μL), ethyl acetate (200 μL), acetic anhydride (600 µL), perchloric acid (60 %, 23 µL) and incubating (25 °C, 15 min). Type 1 water (2 mL) and 1-methylimidazole (40  $\mu$ L) were added prior to dichloromethane (DCM, 2 mL) for partitioning. Following mixing and centrifuging (rcf 733, 5 min), the aqueous layer was discarded, and the DCM phase was rinsed with 0.5 M Na<sub>2</sub>CO<sub>3</sub> (2 mL) and Type 1 water (2 mL, twice). Finally, the DCM was evaporated under a stream of air and the residual PMAAs dissolved in acetone (analytical grade) for analysis.

PMAAs were analysed on an Agilent 8890 GC system coupled with a 5977B mass selective detector. Samples (1  $\mu L)$  were auto-injected at 250 °C, using splitless mode, onto a BPX90 fused-silica capillary column (25 m  $\times$  0.22 mm i.d., 0.25 mm film thickness) at 80 °C with a He flow rate of 1.5 mL min $^{-1}$ . The temperature was held for 1 min before increasing to 130 °C at 50 °C min $^{-1}$ , then to 250 °C at 5 °C min $^{-1}$  with a final hold of 10 min. The separated derivatives were analysed using an electron impact mass detector (70 eV, source temperature 230 °C, quadrupole temperature 150 °C), scanning from 40 to 400 m/z. Data were processed in Agilent OpenLabs software (Ver. 2.4).

#### 2.3. NMR spectroscopy

Native and desulfated (80 °C or 100 °C) ulvans were D<sub>2</sub>O exchanged three times before being made up to a final concentration of 25 mg mL<sup>-1</sup>. Acetone (0.1%v/v) was added as an internal standard to all samples and assigned as the reference peak (31.45 ppm <sup>13</sup>C and 2.225 ppm <sup>1</sup>H). NMR data was collected on a 500 MHz Jeol type JNM-ECZ500R/S1 NMR operating at a proton frequency of 500.160 MHz with a two channel 5-mm FG/RO Digital auto tune Royal probe. Spectra were acquired at 70 °C following 120 s of equilibration once temperature was reached; pw90 values for proton and carbon were re-calibrated for optimum values at 70  $^{\circ}$ C. Proton NMR spectra were recorded with a spectral width of 10 ppm, 32,768 complex data points, resolution of 0.19 Hz, 45-degree excitation pulse, each with a 5 s delay time and an acquisition time of 5.24 s. Heteronuclear single quantum coherence (HSQC) experiments were carried out using the pulse program hsqc\_dec\_phase\_pfgzz (absorption pfg zz filter hsqc with x-decoupling) supplied by Jeol. NMR chemical shifts were assigned based on the literature sources detailed in Kidgell et al. (2021) (de Carvalho et al., 2018; de Freitas et al., 2015; Lahaye, Inizan, & Vigouroux, 1998; Reisky et al., 2019).

#### 2.4. Data analysis

PMAAs were identified by GC retention time relative to the internal standard *myo*-inositol and from electron impact mass spectra, compared to previously prepared PMAA standards and online resources (https://gl

ygen.ccrc.uga.edu/ccrc/specdb/ms/pmaa/pframe.html) (Doares, Albersheim, & Darvill, 1991; Glasson et al., 2022). The relative mol% of individual PMAA derivatives was calculated by standardising the peak area by the respective molecular mass of the derivative.

FTIR figures were produced using R Studio (Ver. 1.4) from data exported from Opus (Ver. 8.1). Figures produced in propriety software were refined in Adobe Illustrator (Ver. 24) and Inkscape (Ver. 1.1).

NMR spectra were analysed and processed in MestreNova (Ver. 14.2.1). Processing included reducing T1 noise, manual phase correction using the methyl peak of rhamnose as pivot, auto-baseline correction, normalising intensity to the rhamnose methyl peak as a value of 100, referencing chemical shift to acetone internal standard, and, if necessary, denoise by VOI compression (Puig-Castellví, Pérez, Piña, Tauler, & Alfonso, 2018).

#### 3. Results

The glycosyl linkage compositions of the carboxyl reduced native ulvan (NAT) and 80 °C and 100 °C desulfated ulvans (DS80, DS100) prepared from each of the four *Ulva* species are shown in Table 1. The major constituent monosaccharides, rhamnose (Rha), glucuronic acid (GlcA), xylose (Xyl), iduronic acid (IdoA), and galactose (Gal), were all predominantly 4-linked (Table 1). Rha and GlcA residues dominated the composition of all four ulvans, accounting for 68–87 mol% of NAT ulvans, consistent with the results from HPAEC-PAD constituent sugar analysis (Table 2). Comparison of the glycosyl linkage compositions of native ulvans (NAT) with their desulfated counterparts (DS80 and DS100) indicated that 4-linked Rha is predominantly 3-O-sulfated in all four ulvans (Table 1, Fig. 1). Additionally, the linkage analysis suggests that some 4-linked Xyl is 2-O-sulfated in all four ulvans, and that minor proportions of 4-linked GlcA may be 2-O-sulfated in the ulvans from tubular species.

The ulvans from foliose and tubular species of *Ulva* had distinctly different glycosyl linkage compositions, as discussed below.

#### 3.1. Foliose species: U. stenophylloides and U. lacinulata

The predominant glycosyl linkages of NAT ulvans from the foliose species, U. stenophylloides and U. lacinulata, were  $\rightarrow 3,4$ )-Rhap- $(1\rightarrow$  and  $\rightarrow 4$ )-GlcAp- $(1\rightarrow$ , with lower proportions of  $\rightarrow 4$ )-IdoAp- $(1\rightarrow$  also present (Table 1). These glycosyl linkages comprised 81 and 67 mol% of the total linkages from U. stenophylloides and S0. stenophylloides and S1. stenophylloides and S2. stenophylloides and S3. stenophylloides and S4. stenophylloides and S5. stenophylloides and S6. stenophylloides and S6. stenophylloides and S7. stenophylloides and S8. stenophylloides

The position of sulfate esters on constituent monosaccharides was determined by monitoring the change in proportion of glycosyl linkages between native and desulfated ulvans. A reduction in proportion of O-3 linkages during desulfation indicates that the majority of 4-linked Rha residues in ulvan from U. stenophylloides were sulfated. There was a progressive loss of the 3-O-sulfate esters between NAT, DS80, and DS100 ulvans as evidenced by the successive decrease in the proportion of  $\rightarrow$ 3,4)-Rhap-(1 $\rightarrow$  from 44, to 34, to 13 mol%, respectively, with a simultaneous increase in the proportion of  $\rightarrow$ 4)-Rhap-(1  $\rightarrow$  from 2, to 10, to 31 mol%. A small proportion of 3-O-sulfate esters remaining in DS100 ulvan was expected due to incomplete desulfation (see supplementary data). The loss of 3-O-sulfate esters from Rha was supported by  $^{1}H^{-13}C$ HSQC NMR spectra of native and 100 °C desulfated ulvan from U. stenophylloides (Fig. 1, Figs. S4-S6). The HSQC spectrum of desulfated ulvan had a resonance at <sup>13</sup>C 71.7 ppm / <sup>1</sup>H 3.94 ppm (Fig. 1, Table S2), where a non-sulfated C3/H3 of Rha was expected (Reisky et al., 2019). This resonance was absent in the HSQC spectrum of the native ulvan (Fig. 1), suggesting the majority of C3 of Rha was sulfated. Desulfation at  $100\,^{\circ}\text{C}$  showed changes in other resonances, particularly in the anomeric region, probably as a result of the loss of 3-O-sulfate esters from Rha. The inverse change in proportion of  $\rightarrow 2,4$ )-Xylp-(1  $\rightarrow$  to  $\rightarrow 4$ )-Xylp-(1  $\rightarrow$  and  $\rightarrow$ 3)-Rhap-(1  $\rightarrow$  to Rhap-(1 $\rightarrow$ , between native and desulfated ulvans

Table 1 Glycosyl linkage composition (relative mol%, average of duplicate analyses) of the carboxyl reduced native (NAT) and desulfated (80 °C and 100 °C; DS80 and DS100, respectively) ulvans isolated from U. S see supplementary Table S1 for the complete data set.

		U. steno	phylloides		U. lacin	ulata		U. ralfsi	i		U. prolij	era	_
Derivative	Deduced Linkage	NAT	DS80	DS100	NAT	DS80	DS100	NAT	DS80	DS100	NAT	DS80	DS100
2,3,4-Rha <sup>a</sup>	Rhap-(1→	_b	1.2	1.9	2.4	2.4	3.0	3.0	3.0	3.3	16.9	15.0	17.7
2,4-Rha	$\rightarrow$ 3)-Rhap-(1 $\rightarrow$	1.7	1.4	_	3.4	1.4	_	2.2	2.2	1.8	7.2	8.0	7.7
2,3-Rha	$\rightarrow$ 4)-Rhap-(1 $\rightarrow$	1.9	9.9	31.3	4.6	10.7	28.6	-	3.1	8.4	3.0	7.0	10.8
3-Rha	$\rightarrow$ 2,4)-Rhap-(1 $\rightarrow$	-	1.1	3.2	-	1.3	3.5	-	6.4	16.1	-	4.3	11.4
2-Rha	$\rightarrow$ 3,4)-Rhap-(1 $\rightarrow$	43.8	34.0	13.0	35.8	32.5	14.8	13.3	9.3	5.1	17.0	12.8	6.6
Rha	$\rightarrow$ 2,3,4)-Rhap-(1 $\rightarrow$	6.0	4.8	1.7	10.4	5.8	3.1	23.5	15.5	7.0	20.9	16.3	8.4
	Total Rha	53.4	52.3	51.1	56.5	53.9	53.1	42.0	39.6	41.6	64.9	63.4	62.6
2,3,4,6-Glc	$GlcAp$ - $(1 \rightarrow$	-	1.2	_	1.9	_	_	-	_	_	-	_	_
2,3,6-Glc	$\rightarrow$ 4)-GlcAp-(1 $\rightarrow$	31.4	31.2	32.9	22.1	24.1	25.4	21.6	24.8	24.5	9.7	10.6	11.9
3,6-Glc	$\rightarrow$ 2,4)-GlcAp-(1 $\rightarrow$	-	-	_	_	-	_	3.6	2.0	_	4.7	4.2	3.2
2,6-Glc	$\rightarrow$ 3,4)-GlcAp-(1 $\rightarrow$	-	-	_	_	-	_	-	-	_	1.4	1.3	1.2
	Total GlcA	31.4	32.4	32.9	24.0	24.1	25.4	25.2	26.9	24.5	15.7	16.0	16.3
2,3-Xyl	$\rightarrow$ 4)-Xylp-(1 $\rightarrow$	3.8	6.3	7.0	5.0	6.0	6.2	10.2	12.3	13.9	6.5	9.8	11.5
3-Xyl	$\rightarrow$ 2,4)-Xylp-(1 $\rightarrow$	1.6	_	_	1.3	_	_	3.1	2.4	2.1	4.7	3.1	2.5
-	Total Xyl	5.4	6.3	7.0	6.3	6.0	6.2	13.3	14.8	15.9	11.2	12.9	14.0
2,3,6-Ido	$\rightarrow$ 4)-IdoAp-(1 $\rightarrow$	5.8	6.9	7.0	9.1	12.5	13.2		1.6	2.0	2.5	2.6	3.0
	Total IdoA	5.8	6.9	7.0	9.1	12.5	13.2	0.0	1.6	2.0	2.5	2.6	3.0
2,3,4,6-Gal	$Galp-(1\rightarrow$	-	_	_	_	_	_	-	1.2	2.6	-	_	_
2,3,6-Gal	$\rightarrow$ 4)-Galp-(1 $\rightarrow$	-	_	_	_	_	_	13.3	12.0	9.1	-	_	_
2,3,4-Gal	$\rightarrow$ 6)-Galp-(1 $\rightarrow$	_	_	_	1.0	1.1	1.1	_	1.5	2.0	1.2	2.4	2.5
2,6-Gal	$\rightarrow$ 3,4)-Galp-(1 $\rightarrow$	_	_	_	1.3	_	_	1.5	_	_	2.3	-	_
2,3-Gal	$\rightarrow$ 4,6)-Galp-(1 $\rightarrow$	_	-	_	_	_	_	1.0	-	_	_	_	_
	Total Gal	0.0	0.0	0.0	2.4	1.1	1.1	15.8	14.6	13.7	3.5	2.4	2.5
	Others <sup>c</sup>	3.9	2.1	2.1	1.7	2.3	1.0	3.7	2.5	2.2	2.3	2.7	1.7

 $<sup>^{\</sup>rm a}$  2,3,4-Rha = 1,5-di-O-acetyl-1-deuterio-2,3,4-tri-O-methylrhamnitol etc.

**Table 2**Constituent sugar composition (normalised mol%) of native ulvan from *U. stenophylloides, U. lacinulata, U. ralfsii,* and *U. prolifera* quantified by HPAEC-PAD. See Kidgell et al. (2021) for details.

	Ulvan species							
Sugar	U. stenophylloides (cult.B)	U. lacinulata	U. ralfsii (cult.)	U. prolifera				
Rha	48 <sup>a</sup>	49	38	60				
GlcA	31	26	24	17				
Xyl	7	6	16	15				
IdoA	11	18	4	7				
Gal	2	tr. <sup>b</sup>	16	tr.				

<sup>&</sup>lt;sup>a</sup> Values are the averages of duplicate analyses.

from both foliose species, suggest the presence of 2-O-sulfate on some of the Xyl and a 3-O-sulfate on terminal Rha (Table S1). The glycosyl linkage compositions of ulvan from U. lacinulata indicated the majority of  $\rightarrow$ 4)-Rhap-(1  $\rightarrow$  residues were also 3-O-sulfated, although the higher proportion of  $\rightarrow$ 2,3,4)-Rhap-(1  $\rightarrow$  in this ulvan generally complicates interpretation of both the linkage analysis data and NMR spectra (Figs. S3, S7-S10).

The NAT ulvans from U. stenophylloides and U. lacinulata contained 6.0 and 10.4 mol% of  $\rightarrow 2,3,4$ )-Rhap- $(1\rightarrow$  (fully substituted Rha), respectively (Table 1). Assuming minimal undermethylation has occurred and the O-3 position of Rha is predominantly sulfated, the presence of  $\rightarrow 2,3,4$ )-Rhap- $(1\rightarrow$  in the glycosyl linkage compositions of NAT ulvans indicates the O-2 of a portion of  $\rightarrow 4$ )-Rhap- $(1\rightarrow$  residues must be either sulfated, glycosidically linked to another sugar, or substituted with another functional group. As observed with  $\rightarrow 3,4$ )-Rhap- $(1\rightarrow$ , there was a progressive decrease in the proportion of  $\rightarrow 2,3,4$ )-Rhap- $(1\rightarrow$  between NAT, DS80, and DS100 ulvans from both species, suggesting 3-O and/or 2-O-sulfation. Comparing the net change in linkage proportions between NAT and DS100 ulvans for each species provides an indication of the extent of sulfation (Table 3). For U.

stenophylloides, two thirds of the reduction in  $\rightarrow$ 2,3,4)-Rhap-(1 $\rightarrow$  is accounted for by an increase in  $\rightarrow$ 2,4)-Rhap-(1 $\rightarrow$  (Table 3), while only half of the reduction in  $\rightarrow$ 2,3,4)-Rhap-(1 $\rightarrow$  is accounted for by  $\rightarrow$ 2,4)-Rhap-(1 $\rightarrow$  in *U. lacinulata* (Table 3). These trends suggest there may be some minor sulfation at the *O*-2 position in addition to the expected *O*-3 sulfation. Sulfation at the *O*-2 position of Rha in ulvan from *U. lacinulata* is further supported by the fact that there is a higher proportion of  $\rightarrow$ 4)-Rhap-(1 $\rightarrow$  produced from desulfation at 100 °C than can be accounted for by the reduction in  $\rightarrow$ 3,4)-Rhap-(1 $\rightarrow$  residues in DS100 ulvan not accounted for by a reduction in  $\rightarrow$ 3,4)-Rhap-(1 $\rightarrow$ , and 3.8 mol% of  $\rightarrow$ 2,3,4)-Rhap-(1 $\rightarrow$  not accounted for by an increase in  $\rightarrow$ 2,4)-Rhap-(1 $\rightarrow$ , suggesting that some of the  $\rightarrow$ 2,3,4)-Rhap-(1 $\rightarrow$  may be 2,3-disulfated.

### 3.2. Tubular species: U. ralfsii and U. prolifera

The NAT ulvan of tubular *U. ralfsii* predominantly contained fully substituted rhamnose,  $\rightarrow 2,3,4$ )-Rhap- $(1\rightarrow$ , and  $\rightarrow 4$ )-GlcAp- $(1\rightarrow$  (45.1) mol% combined), while NAT ulvan of *U. prolifera* was mainly composed of  $\rightarrow 2,3,4$ )-Rhap- $(1\rightarrow, \rightarrow 3,4)$ -Rhap- $(1\rightarrow, and terminal Rhap-<math>(1\rightarrow, 54.8)$ mol% combined) (Table 1). There was a greater variety of linkages detected in the ulvans from the two tubular species compared to the two foliose species (U. stenophylloides and U. lacinulata) reported in the previous section. Where  $\rightarrow$ 3,4)-Rhap-(1 $\rightarrow$ ,  $\rightarrow$ 4)-GlcAp-(1 $\rightarrow$ , and $\rightarrow$ 4)-IdoAp-(1→ accounted for 81 and 67 mol% of linkages of NAT ulvan from U. stenophylloides and U. lacinulata, respectively, these residues only accounted for 35.9 and 29.2 mol% of NAT ulvan of U. ralfsii and U. prolifera, highlighting the difference in ulvan composition from different Ulva morphologies. The NMR spectra collected from U. ralfsii and U. prolifera ulvans were not diagnostic for structure and sulfation patterns due to low resonance intensity (Figs. S11-S18). However, there were features of the spectra that highlighted the differences in the structure of the ulvans from these tubular species compared with the foliose species. In addition to the resonances for the primary disaccharide units, A3s [ $\rightarrow$ 4)- $\beta$ -D-GlcpA-(1 $\rightarrow$ 4)- $\alpha$ -L-Rhap3S-(1 $\rightarrow$ ], B3s [ $\rightarrow$ 4)- $\alpha$ -L-

<sup>&</sup>lt;sup>b</sup> -, not detected.

<sup>&</sup>lt;sup>c</sup> Other minor linkages <1 mol%.

b Sugars <1 mol% are considered trace (tr.)</p>

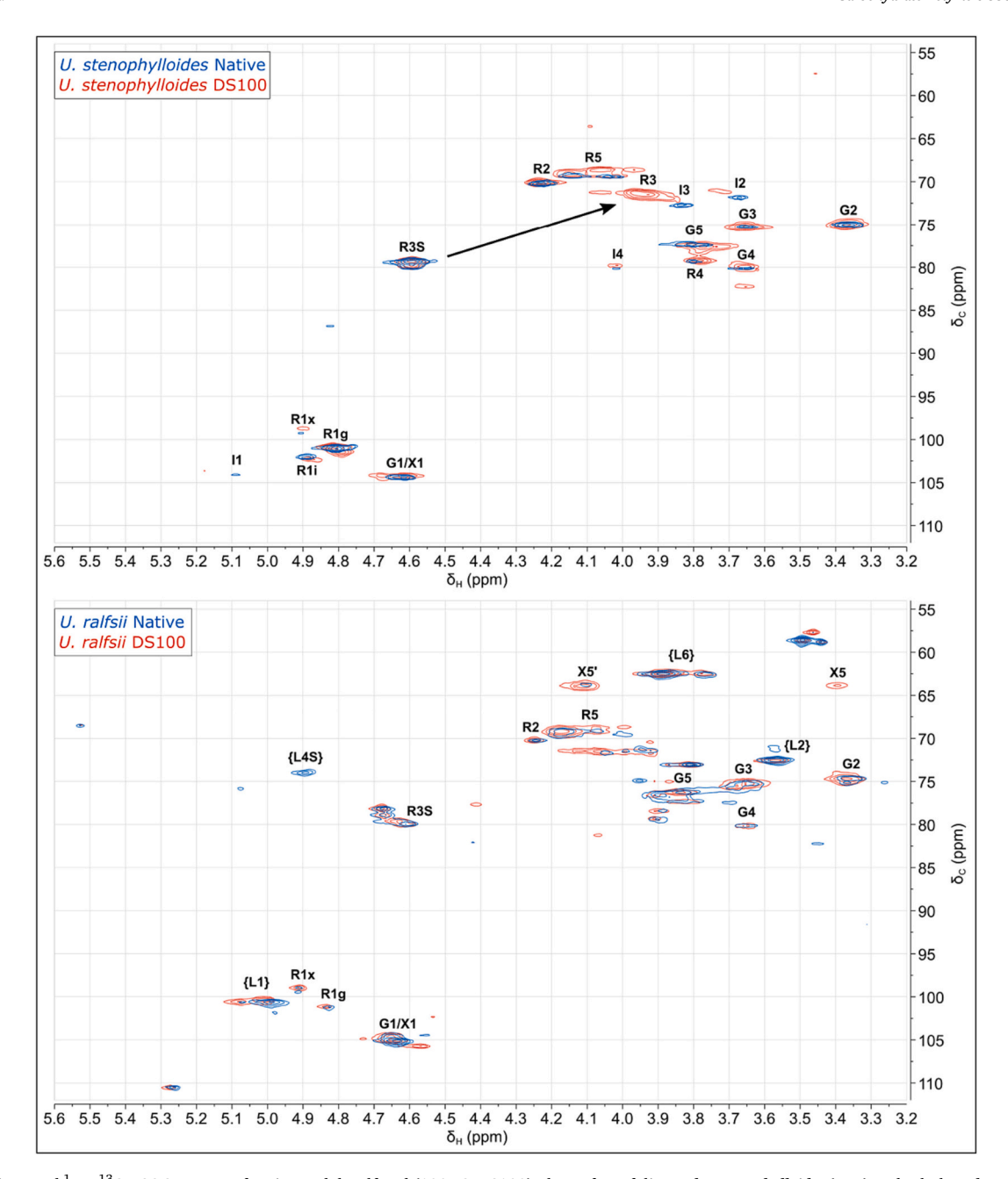


Fig. 1. Superimposed  $^1H^{-13}C$  HSQC spectra of native and desulfated (100  $^{\circ}C$ , DS100) ulvans from foliose *Ulva stenophylloides* (Top) and tubular *Ulva ralfsii* (Bottom). The arrow indicates the shift in resonance of C3-H3 of rhamnose due to desulfation. Labels and numbers correspond to carbon/proton coupling pair of ulvan units: G and R = GlcpA and Rhap3S of A<sub>36</sub>; I and Ri = IdopA and Rhap3S of B<sub>36</sub>; X and Rx = Xylp and Rhap3S of U<sub>36</sub>; L = tentative assignments of galactose based on literature and intensity of resonances. Non-superimposed HSQCs from all derivatised ulvans are in the supplementary data. Chemical shifts relative to acetone at 31.45 and 2.225 ppm for  $^{13}C$  and  $^{1}H$ , respectively; intensities normalised to the rhamnose methyl peak ( $\sim$ 18.1 ppm  $^{13}C$  and  $\sim$ 1.30 ppm  $^{1}H$ ).

IdopA-(1→4)-α-L-Rhap3S-(1→] and U3s [→4)-β-D-Xylp-(1→4)-α-L-Rhap3S-(1→] observed in ulvans from both foliose and tubular species, the HSQC spectra from *U. ralfsii* and *U. prolifera* ulvans had anomeric resonances at  $^{13}$ C 100.1–103.1 ppm /  $^{1}$ H 4.98–5.09 ppm. These resonances were tentatively assigned to α-Gal residues based on literature (Maurya et al., 2023; Zavadinack et al., 2021). In addition, a resonance observed at  $^{13}$ C 110.6 ppm /  $^{1}$ H 5.26 ppm was tentatively assigned to a Galf residue (Arata, Quintana, Raffo, & Ciancia, 2016; Capek et al., 2020). Resonances at  $^{13}$ C 57.6–58.8 ppm /  $^{1}$ H 3.44–3.49 ppm assigned to methoxy substituents, such as 3-O-Me rhamnose, were more intense in the two tubular species than the foliose species (Kidgell et al., 2021).

The degree and position of sulfation was also different in ulvans from tubular species of *Ulva* compared to foliose species. There was twice the

relative mol% of Xyl in ulvans from tubular species, *U. ralfsii* and *U. prolifera*, compared to foliose species (Table 1, Table 2), which was mostly present as  $\rightarrow$ 4)-Xylp-(1 $\rightarrow$  with lower proportions of  $\rightarrow$ 2,4)-Xylp-(1 $\rightarrow$  that decreased with desulfation (Table S1), indicating possible 2-*O*-sulfation. Small proportions of glucuronic acid in both ulvans may also be sulfated at *O*-2, as evidenced by the minor proportions of  $\rightarrow$ 2,4)-GlcAp-(1 $\rightarrow$  decreasing due to desulfation with a concomitant increase in  $\rightarrow$ 4)-GlcAp-(1 $\rightarrow$  (Table 1, Table S1). With respect to the Rha residues, *U. ralfsii* NAT and DS100 ulvans had near equal stoichiometric ratios of  $\rightarrow$ 3,4)-Rhap-(1 $\rightarrow$  to  $\rightarrow$ 4)-Rhap-(1 $\rightarrow$  and  $\rightarrow$ 2,3,4)-Rhap-(1 $\rightarrow$  to  $\rightarrow$ 2,4)-Rhap-(1 $\rightarrow$  (Table 3), indicating that Rha in this ulvan was exclusively 3-*O*-sulfated. While the ratio of  $\rightarrow$ 2,3,4)-Rhap-(1 $\rightarrow$  to  $\rightarrow$ 2,4)-Rhap-(1 $\rightarrow$  in *U. prolifera* was almost equal, the increase in  $\rightarrow$ 4)-Rhap-(1 $\rightarrow$  during

#### Table 3

The stoichiometric change of rhamnose glycosyl linkages from native (NAT) ulvans isolated from U. stenophylloides, U. lacinulata, U. ralfsii, and U. prolifera that were 100 °C desulfated (DS100). Values were calculated from the data presented in Table 1 by subtracting the relative mol% of glycosyl linkages for DS100 ulvans from corresponding NAT ulvans. A positive value indicates an increase in the occurrence of a linkage residue with desulfation and a negative value indicates a decrease in occurrence.

	Net stoichiometric change in mol% between NAT and DS100 ulvans							
Deduced Linkage	U. stenophylloides	U. lacinulata	U. ralfsii	U. prolifera				
Rhap-(1→	1.9 <sup>a</sup>	0.6	0.3	0.8				
$\rightarrow$ 3)-Rha $p$ -(1 $\rightarrow$	-1.7	-3.4	-0.4	0.5				
$\rightarrow$ 4)-Rhap-(1 $\rightarrow$	29.4	24	8.4	7.8				
$\rightarrow$ 2,4)-Rhap-(1 $\rightarrow$	3.2	3.5	16.1	11.4				
$\rightarrow$ 3,4)-Rhap-(1 $\rightarrow$	-30.8	-21	-8.2	-10.4				
$\rightarrow$ 2,3,4)-Rhap-(1 $\rightarrow$	-4.3	-7.3	-16.5	-12.5				
Total Rha	-2.3	-3.4	-0.4	-2.3				

<sup>&</sup>lt;sup>a</sup> 'Not detected' values were considered "0" for calculations.

desulfation only accounted for three quarters of the decrease in  $\rightarrow$ 3,4)-Rhap-(1 $\rightarrow$  between NAT and DS100 ulvans (Table 3). The source of this discrepancy is unclear but may involve the large proportion of Rhap-(1 $\rightarrow$  detected in ulvan from *U. prolifera* (Table 1).

The ulvan from *U. prolifera* contained greater proportions of terminal rhamnose (Rhap- $(1\rightarrow, 15-18 \text{ mol}\%)$  and  $\rightarrow 3$ )-Rhap- $(1\rightarrow (7-8 \text{ mol}\%)$ than ulvans from the other species examined or reported in the literature (Table 1). These residues help explain the unusually high proportion of rhamnose (60 mol%) previously detected by constituent sugar analysis (Table 2). The high proportion of galactose detected in the NAT ulvan isolated from *U. ralfsii* (16 mol%; Table 1, Table 2) was predominantly  $\rightarrow$ 4)-Galp-(1 $\rightarrow$  (13 mol%), with minor proportions of Galp-(1 $\rightarrow$ ,  $\rightarrow$ 6)- $Galp-(1\rightarrow, \rightarrow 3,4)-Galp-(1\rightarrow, and \rightarrow 4,6)-Galp-(1\rightarrow (Table 1, Table S1).$ Comparing NAT and desulfated ulvans from U. ralfsii indicate that the  $\rightarrow$ 6)-Galp-(1 $\rightarrow$  may be partially O-4 sulfated (Table S1). The loss of 4-Osulfate esters from Gal was tentatively supported by <sup>1</sup>H—-<sup>13</sup>C HSQC NMR spectra of native and 100 °C desulfated ulvans from U. ralfsii and U. prolifera (Fig. 1, Figs. S12-S18). The HSQC spectrum of the native ulvans had a resonance at <sup>13</sup>C 73.9 ppm / <sup>1</sup>H 4.89 ppm, which was absent in the HSQC spectrum of the desulfated ulvans (Bilan, Vinogradova, Shashkov, & Usov, 2007; Farias, Valente, Pereira, & Mourão, 2000). Partial 4-O-sulfation of terminal galactose residues could also explain the reduction of  $\rightarrow 4$ )-Galp-(1  $\rightarrow$  with increasing desulfation and the concomitant increase in the proportion of Galp- $(1 \rightarrow \text{(Table 1},$ Table S1).

#### 4. Discussion

This study is a detailed investigation of the glycosyl linkage compositions of ulvans from multiple species of Ulva. The carbohydrate composition, linkage pattern and sulfate ester positions on constituent monosaccharides of ulvans isolated from foliose (U. lacinulata and U. stenophylloides) and tubular (U. prolifera and U. ralfsii) species of Ulva were investigated. The positions of sulfate esters were determined by comparing the linkage compositions of native ulvans (NAT) to desulfated ulvans (DS80 and DS100). The results confirm that all four ulvans studied were consistent with the literature consensus of the ulvan polysaccharide containing a 4-linked backbone of GlcA, IdoA, Xyl, and 3-O-sulfated Rha (Chattopadhyay et al., 2007; Glasson et al., 2022; Lahaye & Robic, 2007; Lopes et al., 2017; McKinnell & Percival, 1962; Ray & Lahaye, 1995). However, the results also highlighted the disparity in glycosyl linkage proportions between ulvans from the different morphologies of Ulva. Ulvans from foliose species were predominantly 4-linked GlcA/IdoA and 3-O-sulfated Rha. While ulvans from tubular species also contained high proportions of 4-linked GlcA and 3-Osulfated Rha, there was also a substantially higher proportion of other

glycosyl linkage residues. In addition to the majority of Rha being 3-O-sulfated in all the ulvans examined, there was also evidence of low levels of 2,3-disulfation in Rha residues in ulvan of foliose species and sulfation on Xyl and GlcA residues in ulvans from tubular species. Further, NMR data showed that tubular species contained greater proportions of methoxy substitution than foliose species. These results confirm our hypothesis that, among the ulvans studied here, those from tubular species of *Ulva* are more complex in structure.

The simpler structure of ulvans from foliose species can be inferred from the higher proportions of limited glycosyl linkages, while ulvans from tubular species contained a higher diversity of glycosyl linkages. The glycosyl linkages of the  $A_{3S}$  disaccharide (  $\rightarrow 4)\text{-}GlcAp\text{-}(1\rightarrow \text{ and }$  $\rightarrow$ 3,4)-Rhap-(1 $\rightarrow$ ) and B<sub>3S</sub> disaccharide ( $\rightarrow$ 4)-IdoAp-(1 $\rightarrow$  and  $\rightarrow$ 3,4)-Rhap- $(1\rightarrow)$  account for 81 % and 67 % of the linkages for NAT ulvan from foliose *U. stenophylloides* and *U. lacinulata*, respectively. Such high proportions of A<sub>3S</sub> and B<sub>3S</sub> disaccharides suggests that ulvans of foliose species are predominantly linear (unbranched) sections of repeat disaccharide units, as has been reported for ulvan (Lahaye & Robic, 2007; Paradossi, Cavalieri, & Chiessi, 2002). In contrast, the same three residue components comprising the A<sub>3S</sub> and B<sub>3S</sub> disaccharides only account for 36 % and 29 % of NAT ulvans from tubular U. ralfsii and *U. prolifera*, respectively. Even with the inclusion of  $\rightarrow 4$ )-Xylp-(1 $\rightarrow$  and  $\rightarrow$ 2,4)-Xylp-(1 $\rightarrow$  (respectively representing the U<sub>3S</sub> and U<sub>2S'3S</sub> disaccharides in combination with Rha-3-sulfate) only 48 % and 38 % of the residues in the ulvans from U. ralfsii and U. prolifera are accounted for, respectively. The greater complexity of ulvans in tubular species of Ulva can also be inferred from the NMR spectra collected. Despite the samples of ulvan for foliose and tubular species being prepared and run identically, there are a higher number of low intensity resonances in the <sup>1</sup>H—<sup>13</sup>C HSQC spectra for ulvans of tubular species (Figs. S12-S18) compared to the lower number of high intensity resonances for ulvans of foliose species (Figs. S4-S10). Size-exclusion chromatography coupled with multi-angle laser light scattering shows that ulvans from U. ralfsii (tubular) and U. stenophylloides (foliose) have similar elution volumes, but the U. ralfsii ulvan has a much higher molecular weight (Kidgell et al., 2021). This indicates that the *U. ralfsii* ulvan has a more compact, branched structure which is consistent with the greater complexity observed in the NMR spectra.

A uniting feature of all four NAT ulvans was that over 90 % of 1,4-linked rhamnose were 3-O substituted, which reduced to 30–40 % following 100 °C desulfation; clear evidence for the majority of rhamnose in native ulvan being 3-O-sulfated. At least some 3-O substitution was expected on desulfated Rha as the desulfation procedure did not run to completion in this experiment (see supplementary data). The authors acknowledge that this is a limitation to the study, but as the desulfation method employed eventually caused depolymerisation of the polysaccharide (Fig. S2), structural integrity was prioritised over complete liberation of the sulfate esters. The authors also note that the IdoA content observed from glycosyl linkage analysis (Table 1) was approximately half of what was detected in constituent sugar analysis by HPAEC-PAD (Table 2) for all ulvans. This reduction may be due to the acid lability of iduronic acid (Conrad, 1980) and the additional derivatisation steps required for glycosyl linkage analysis.

All four ulvans also contained varying proportions of  $\rightarrow 2,3,4$ )-Rhap- $(1\rightarrow$ . The presence of a fully substituted sugar like  $\rightarrow 2,3,4$ )-Rhap- $(1\rightarrow$  is a characteristic sign that the sugars were undermethylated (Biermann & McGinnis, 1989) during analysis. However, the near-stoichiometric shift of the O-3 substitution of rhamnose from acetyl (sulfated) to methyl (desulfated) as the degree of desulfation increased between NAT, DS80, and DS100 PMAA derivatives (Table 1) indicates complete methylation. In the case of ulvan from U. prolifera, the  $\rightarrow 2,3,4$ )-Rhap- $(1\rightarrow$  could be attributed to 3-O-sulfation combined with O-2 branching to the high proportion of terminal Rhap- $(1\rightarrow$  residues detected. Indeed, the 17 mol % of terminal Rhap- $(1\rightarrow$  residues in DS100 ulvan from U. prolifera almost matches the 21 mol% non-sulfate branches on the other DS100 residues detected (Table 1). In contrast, the combined proportions of

terminal sugars in each of the other DS100 ulvans from the other three *Ulva* species only accounts for one third to one half of the branches present, assuming all *O*-3 substituents on 1,4-linked rhamnose moieties are sulfate esters (Table 1). The exceptionally high proportions of terminal rhamnose (15.0–17.7 mol%) detected in ulvan from *U. prolifera* is a unique finding in the ulvan literature. Generally, only lesser quantities of terminal glucuronic acid (1–8 mol%) and terminal rhamnose (1–3 mol%) are reported for ulvans (Chattopadhyay et al., 2007; Glasson et al., 2022; Gosselin et al., 1964; Ray & Lahaye, 1995).

The more minor occurrences of  $\rightarrow$ 2,3,4)-Rhap-(1 $\rightarrow$  in the ulvans from foliose species may be attributable to minor 2,3-*O*-disulfation, as reported by Glasson et al. (2022). In support of this theory, the increase in proportion of  $\rightarrow$ 2,4)-Rhap-(1 $\rightarrow$  only accounts for three quarters to half of the decrease in  $\rightarrow$ 2,3,4)-Rhap-(1 $\rightarrow$  in the ulvans, and there is a second, unidentified, resonance next to the C3-H3 resonance for 3-*O*-sulfated Rha ( $^{13}$ C 79.4 ppm /  $^{1}$ H 4.59 ppm) on the  $^{1}$ H $^{-13}$ C HSQC spectra for these ulvans (Fig. 1, Figs. S15-S18, Table S3) which could potentially be C2-H2 of 2-*O*-sulfated Rha. Terminal GlcAp-(1 $\rightarrow$  were also detected in the ulvan from foliose species and has been previously reported as a branch on *O*-2 of Rha (Lahaye & Ray, 1996).

The source of the high  $\rightarrow 2,3,4$ )-Rhap- $(1\rightarrow$  residues in ulvan from U. ralfsii is unclear. The stoichiometric shift of  $\rightarrow 2,3,4$ )-Rhap- $(1\rightarrow$  to  $\rightarrow 2,4$ )-Rhap- $(1\rightarrow$  and  $\rightarrow 3,4$ )-Rhap- $(1\rightarrow$  to  $\rightarrow 4$ )-Rhap- $(1\rightarrow$  indicate extensive 3-O-sulfation, but the O-2 substitution on the resulting  $\rightarrow 2,4$ )-Rhap- $(1\rightarrow$  cannot be assigned.

The high proportion of galactose detected in ulvan from U. ralfsii (17 mol%) occurred predominantly as  $\rightarrow$ 4)-Galp-(1 $\rightarrow$ , with minor proportions of Galp- $(1\rightarrow, \rightarrow 6)$ -Galp- $(1\rightarrow, \rightarrow 3,4)$ -Galp- $(1\rightarrow, \text{and } \rightarrow 4,6)$ -Galp- $(1\rightarrow. Ulvan samples from tubular U. tepida and U. prolifera have been$ reported to have similarly high proportions of galactose (13.8 mol% and 27.1 mol%, respectively) in a wide range of glycosyl residues, the most common being  $\rightarrow$ 4)-Galp-(1  $\rightarrow$  and  $\rightarrow$ 3,4)-Galp-(1  $\rightarrow$  (Glasson et al., 2022). Despite not being considered a major constituent of ulvan, high proportions (7-27 mol%) of galactose are commonly detected in ulvans from tubular species of Ulva (e.g., U. compressa, U. intestinalis, and U. linza) (Chattopadhyay et al., 2007; Glasson et al., 2022; Kidgell et al., 2021; Lopes et al., 2017; Matloub et al., 2016; Qi et al., 2013; Ray, 2006; Tabarsa, You, Dabaghian, & Surayot, 2018). These high proportions of galactose are well in excess of the literature median of 2.1 mol% (Kidgell et al., 2019). However, it is important to note that this median is produced from literature where over 75 % of the data is related to ulvans from foliose species of *Ulva*. Ulvans from foliose species consistently report low proportions of galactose. For example, assessment of the composition of 19 ulvans from five foliose species (U. armoricana, U. lacinulata, U. rotundata, U. scandinavica, and U. olivascens) collected at different times and locations found that galactose ranged from 1.0 to 3.1 mol% (Lahaye et al., 1999).

The source of the galactose in *U. ralfsii* could potentially be from an entrained microorganism. Dinoflagellates of the *Gymnodinium* genus are known to contain sulfated galactans (Hasui, Matsuda, Yoshimatsu, & Okutani, 1995) and be present in New Zealand waters (MacKenzie, 2014). Co-extracted sulfated galactans from such a microorganism would be very difficult to separate from sulfated ulvans by the methods employed in this paper. However, the collected *Ulva* samples were carefully sorted by hand and rinsed prior to mono-cultivation, and genetic barcoding clearly identified *U. ralfsii* without any confounding genetic material present (Lawton et al., 2021). Therefore, it is unlikely that the source of galactose is due to another organism. But further research is needed to determine the role of galactose in ulvan, or if it is a contaminant. Based on the literature and the data collected within this paper, it appears that high proportions of galactose are a unique, yet not ubiquitous, component of ulvans from tubular species of *Ulva*.

#### 5. Conclusion

The glycosyl linkage compositions of the four ulvans assessed

confirm that constituent monosaccharides are predominantly 1,4-linked and that the vast majority of rhamnose is 3-O-sulfated. There were multiple distinct differences between the ulvans from foliose and tubular species of Ulva. Ulvan from tubular species exhibited a more branched structure and a greater diversity of sulfate ester substitution positions, while the ulvans from foliose species closely resembled the literature definition of ulvan structure (Lahaye & Robic, 2007). The predominance of  $\rightarrow 2,3,4$ )-Rhap-(1 $\rightarrow$  in ulvans from tubular species suggests extensive O-2 substitution, likely due to rhamnose side chains in ulvan from U. prolifera and to an unknown target in U. ralfsii. Additionally, minor proportions of sulfate esters detected on O-2 of 1,4-linked glucuronic acid for ulvans from tubular species further highlight the differences between ulvans of different Ulva morphologies. Ulvan from foliose species have a more consistent (likely linear) structure and have been more thoroughly studied. In contrast, ulvans from tubular species have a more complex structure that likely contributes to the higher molecular weight and gelling capacity observed in Kidgell et al. (2021). Ulvans from tubular species are also less thoroughly studied and may have different biological activities compared to ulvans from foliose species. These results support the hypothesis that ulvans from tubular species of Ulva have more complex structure than those from foliose species and highlight the importance of considering the morphology of *Ulva* in ulvan applications.

#### CRediT authorship contribution statement

Joel T. Kidgell: Writing – review & editing, Writing – original draft, Visualization, Investigation, Data curation, Conceptualization. Christopher R.K. Glasson: Writing – original draft, Supervision, Methodology, Investigation, Conceptualization. Marie Magnusson: Writing – review & editing, Resources, Funding acquisition, Conceptualization. Ian M. Sims: Writing – review & editing, Writing – original draft, Investigation. Simon F.R. Hinkley: Writing – review & editing, Supervision, Resources, Funding acquisition, Conceptualization. Susan M. Carnachan: Writing – review & editing, Writing – original draft, Supervision, Investigation, Conceptualization.

## Declaration of competing interest

The authors declare that they have no known competing financial interests or personal relationships that could have appeared to influence the work reported in this paper.

#### Data availability

Data will be made available on request.

#### Acknowledgments

The authors would like to thank Peter Randrup for his assistance with sample collection and *Ulva* cultivation, and Andrew Lewis for his assistance in performing the NMR experiments. We would also like to acknowledge James Cook University and the Australian Government for providing a Research Training Program Scholarship to Joel Kidgell. This research is part of the Entrepreneurial Universities Macroalgal Biotechnologies Programme, jointly funded by the University of Waikato and the Tertiary Education Commission. The authors would also like to thank the Ferrier Research Institute for their assistance and collaboration in this work.

### Appendix A. Supplementary data

Supplementary data to this article can be found online at https://doi.org/10.1016/j.carbpol.2024.121962.

#### References

- Arata, P. X., Quintana, I., Raffo, M. P., & Ciancia, M. (2016). Novel sulfated xylogalactoarabinans from green seaweed Cladophora falklandica: Chemical structure and action on the fibrin network. *Carbohydrate Polymers*, *154*, 139–150.
- Biermann, C. J., & McGinnis, G. D. (1989). Analysis of carbohydrates by GLC and MS. Boca Raton, FL 33431: CRC Press Inc.
- Bilan, M. I., Vinogradova, E. V., Shashkov, A. S., & Usov, A. I. (2007). Structure of a highly pyruvylated galactan sulfate from the Pacific green alga Codium yezoense (Bryopsidales, Chlorophyta). Carbohydrate Research, 342(3-4), 586-596.
- Brading, J. W. E., Georg-Plant, M. M. T., & Hardy, D. M. (1954). The polysaccharide from the alga *Ulva lactuca*. Purification, hydrolysis, and methylation of the polysaccharide. *Journal of the Chemical Society, Resumed*, 319–324.
- Capek, P., Matulová, M., Šutovská, M., Barboríková, J., Molitorisová, M., & Kazimierová, I. (2020). Chlorella vulgaris α-L-arabino-α-L-rhamno-α,β-D-galactan structure and mechanisms of its anti-inflammatory and anti-remodelling effects. International Journal of Biological Macromolecules, 162, 188–198.
- Chattopadhyay, K., Mandal, P., Lerouge, P., Driouich, A., Ghosal, P., & Ray, B. (2007). Sulphated polysaccharides from Indian samples of *Enteromorpha compressa* (Ulvales, Chlorophyta): Isolation and structural features. *Food Chemistry*, 104(3), 928–935.
- Ciucanu, I., & Kerek, F. (1984). A simple and rapid method for the permethylation of carbohydrates. Carbohydrate Research, 131(2), 209-217.
- Conrad, H. E. (1980). The acid lability of the glycosidic bonds of L-iduronic acid residues in glycosaminoglycans. *Biochemical Journal*, 191(2), 355–363.
- de Carvalho, M. M., de Freitas, R. A., Ducatti, D. R. B., Ferreira, L. G., Gonçalves, A. G., Colodi, F. G., et al. (2018). Modification of ulvans via periodate-chlorite oxidation: Chemical characterization and anticoagulant activity. *Carbohydrate Polymers*, 197, 631–640
- de Freitas, M. B., Ferreira, L. G., Hawerroth, C., Duarte, M. E. R., Noseda, M. D., & Stadnik, M. J. (2015). Ulvans induce resistance against plant pathogenic fungi independently of their sulfation degree. *Carbohydrate Polymers*, 133, 384–390.
- Doares, S. H., Albersheim, P., & Darvill, A. G. (1991). An improved method for the preparation of standards for glycosyl-linkage analysis of complex carbohydrates. *Carbohydrate Research*, 210, 311–317.
- Farias, W. R., Valente, A. P., Pereira, M. S., & Mourão, P. A. (2000). Structure and anticoagulant activity of sulfated galactans. Isolation of a unique sulfated galactan from the red algae Botryocladia occidentalis and comparison of its anticoagulant action with that of sulfated galactans from invertebrates. *Journal of Biological Chemistry.*, 275(38), 29299–29307.
- Glasson, C. R. K., Luiten, C. A., Carnachan, S. M., Daines, A. M., Kidgell, J. T., Hinkley, S. F. R., et al. (2022). Structural characterization of ulvans extracted from blade (*Ulva ohnoi*) and filamentous (*Ulva tepida* and *Ulva prolifera*) species of cultivated *Ulva*. *International Journal of Biological Macromolecules*, 194, 571–579.
- Gosselin, C. C., Holt, A., & Lowe, P. A. (1964). Polysaccharides of Enteromorpha species. Journal of the Chemical Society (Resumed), 5877–5880.
- Harris, P. J., Henry, R. J., Blakeney, A. B., & Stone, B. A. (1984). An improved procedure for the methylation analysis of oligosaccharides and polysaccharides. *Carbohydrate Research*, 127(1), 59–73.
- Hasui, M., Matsuda, M., Yoshimatsu, S., & Okutani, K. (1995). Production of a lactate-associated Galactan sulfate by a dinoflagellate *Gymnodinium A<sub>3</sub>*. Fisheries Science, 61 (2), 321–326.
- Hayden, H. S., Blomster, J., Maggs, C. A., Silva, P. C., Stanhope, M. J., & Waaland, J. R. (2003). Linnaeus was right all along: Ulva and Enteromorpha are not distinct genera. European Journal of Phycology, 38(3), 277–294.
- Hughey, J. R., Gabrielson, P. W., Maggs, C. A., & Mineur, F. (2022). Genomic analysis of the lectotype specimens of European Ulva rigida and Ulva lacinulata (Ulvaceae, Chlorophyta) reveals the ongoing misapplication of names. European Journal of Phycology, 57(2), 143–153.
- Kidgell, J. T., Carnachan, S. M., Magnusson, M., Lawton, R. J., Sims, I. M., Hinkley, S. F. R., et al. (2021). Are all ulvans equal? A comparative assessment of the chemical and gelling properties of ulvan from blade and filamentous *Ulva*. *Carbohydrate Polymers*, 264, Article 118010.
- Kidgell, J. T., Glasson, C. R. K., Magnusson, M., Vamvounis, G., Sims, I. M., Carnachan, S. M., et al. (2020). The molecular weight of ulvan affects the in vitro inflammatory response of a murine macrophage. *International Journal of Biological Macromolecules*, 150, 839–848.
- Kidgell, J. T., Magnusson, M., de Nys, R., & Glasson, C. R. K. (2019). Ulvan: A systematic review of extraction, composition and function. Algal Research, 39, Article 101422.
- Lahaye, M., Cimadevilla, E. A. C., Kuhlenkamp, R., Quemener, B., Lognoné, V., & Dion, P. (1999). Chemical composition and 13C NMR spectroscopic characterisation of ulvans from *Ulva* (Ulvales, Chlorophyta). *Journal of Applied Phycology*, 11(1), 1–7.

- Lahaye, M., Inizan, F., & Vigouroux, J. (1998). NMR analysis of the chemical structure of ulvan and of ulvan-boron complex formation. *Carbohydrate Polymers*, 36(2–3), 239–249
- Lahaye, M., & Ray, B. (1996). Cell-wall polysaccharides from the marine green alga *Ulva "rigida"* (Ulvales, Chlorophyta) NMR analysis of ulvan oligosaccharides. Carbohydrate Research, 283, 161–173.
- Lahaye, M., & Robic, A. (2007). Structure and functional properties of ulvan, a polysaccharide from green seaweeds. *Biomacromolecules*, 8(6), 1765–1774.
- Lawton, R., Sutherland, J., Glasson, C., & Magnusson, M. (2021). Selection of temperate Ulva species and cultivars for land-based cultivation and biomass applications. Algal Research, 56, Article 102320.
- Lopes, N., Ray, S., Espada, S. F., Bomfim, W. A., Ray, B., Faccin-Galhardi, L. C., et al. (2017). Green seaweed Enteromorpha compressa (Chlorophyta, Ulvaceae) derived sulphated polysaccharides inhibit herpes simplex virus. International Journal of Biological Macromolecules, 102, 605–612.
- MacKenzie, A. L. (2014). The risk to New Zealand shellfish aquaculture from paralytic shellfish poisoning (PSP) toxins. New Zealand Journal of Marine and Freshwater Research, 48(3), 430–465.
- Matloub, A. A., Aglan, H. A., Mohamed El Souda, S. S., Aboutabl, M. E., Maghraby, A. S., & Ahmed, H. H. (2016). Influence of bioactive sulfated polysaccharide-protein complexes on hepatocarcinogenesis, angiogenesis and immunomodulatory activities. Asian Pacific Journal of Tropical Medicine, 9(12), 1200–1211.
- Maurya, A. K., Sharma, P., Samanta, P., Shami, A. A., Misra, S. K., Zhang, F., et al. (2023). Structure, anti-SARS-CoV-2, and anticoagulant effects of two sulfated galactans from the red alga Botryocladia occidentalis. *International Journal of Biological Macromolecules*, 238, Article 124168.
- McKinnell, J. P., & Percival, E. (1962). Structural investigations on the water-soluble polysaccharide of the green seaweed Enteromorpha compressa. Journal of the Chemical Society (Resumed), 3141–3148.
- Medcalf, D. G., Lionel, T., Brannon, J. H., & Scott, J. R. (1975). Seasonal variation in the mucilaginous polysaccharides from *Ulva lactuca. Botanica Marina*, 18(2), 67–70.
- Nagasawa, K., Inoue, Y., & Tokuyasu, T. (1979). An improved method for the preparation of chondroitin by solvolytic desulfation of chondroitin sulfates. *Journal of Biochemistry*, 86(5), 1323–1329.
- Nelson, W. A., D'Archino, R., Neill, K. F., & Robinson, N. M. (2021). Introduced marine macroalgae: New perspectives on species recognition and distribution in New Zealand. *Botanica Marina*, 64(5), 379–393.
- Nep, E. I., Carnachan, S. M., Ngwuluka, N. C., Kontogiorgos, V., Morris, G. A., Sims, I. M., & Smith, A. M. (2016). Structural characterisation and rheological properties of a polysaccharide from sesame leaves (Sesamun radiatum Schumach. & Thonn.). Carbohydrate Polymers. 152. 541–547.
- Paradossi, G., Cavalieri, F., & Chiessi, E. (2002). A conformational study on the algal polysaccharide ulvan. *Macromolecules*, 35(16), 6404–6411.
- Puig-Castellví, F., Pérez, Y., Piña, B., Tauler, R., & Alfonso, I. (2018). Compression of multidimensional NMR spectra allows a faster and more accurate analysis of complex samples. *Chemical Communications*, 54(25), 3090–3093.
- Qi, X. H., Mao, W. J., Chen, Y., Chen, Y. L., Zhao, C. Q., Li, N., & Wang, C. Y. (2013). Chemical characteristics and anticoagulant activities of two sulfated polysaccharides from Enteromorpha linza (Chlorophyta). Journal of Ocean University of China, 12(1), 175–182
- Ray, B. (2006). Polysaccharides from *Enteromorpha compressa*: Isolation, purification and structural features. *Carbohydrate Polymers*, 66(3), 408–416.
- Ray, B., & Lahaye, M. (1995). Cell-wall polysaccharides from the marine green alga *Ulva* "rigida" (Ulvales, Chlorophyta). Chemical structure of ulvan. *Carbohydrate Research*, 274, 313–318.
- Reisky, L., Préchoux, A., Zühlke, M.-K., Bäumgen, M., Robb, C. S., Gerlach, N., et al. (2019). A marine bacterial enzymatic cascade degrades the algal polysaccharide ulvan. *Nature Chemical Biology*, 15(8), 803–812.
- Sims, I. M., & Bacic, A. (1995). Extracellular polysaccharides from suspension cultures of Nicotiana plumbaginifolia. Phytochemistry, 38(6), 1397–1405.
- Stevenson, T. T., & Furneaux, R. H. (1991). Chemical methods for the analysis of sulphated galactans from red algae. *Carbohydrate Research*, 210, 277–298.
- Tabarsa, M., You, S., Dabaghian, E. H., & Surayot, U. (2018). Water-soluble polysaccharides from *Ulva intestinalis*: Molecular properties, structural elucidation and immunomodulatory activities. *Journal of Food and Drug Analysis*, 26(2), 599–608.
- Usov, A. I., Adamyants, K. S., Miroshnikova, L. I., Shaposhnikova, A. A., & Kochetkov, N. K. (1971). Solvolytic desulphation of sulphated carbohydrates. *Carbohydrate Research*, 18(2), 336–338.
- Zavadinack, M., Bellan, D. L., Bertage, J., Milhorini, S., Trindade, E., Simas, F., et al. (2021). An  $\alpha$ -D-galactan and a  $\beta$ -D-glucan from the mushroom Amanita muscaria: Structural characterization and antitumor activity against melanoma. *Carbohydrate Polymers*, *274*, Article 118647.